BBA - Molecular Basis of Disease 1864 (2018) 3685–3695

Contents lists available at ScienceDirect

BBA - Molecular Basis of Disease

journal homepage: www.elsevier.com/locate/bbadis

IP_3 receptor blockade restores autophagy and mitochondrial function in skeletal muscle fibers of dystrophic mice

Denisse Valladares[a,b,d,*], Yildy Utreras-Mendoza[b], Cristian Campos[b], Camilo Morales[b], Alexis Diaz-Vegas[a,b], Ariel Contreras-Ferrat[a], Francisco Westermeier[a], Enrique Jaimovich[b,c], Saverio Marchi[e], Paolo Pinton[e], Sergio Lavandero[a,b,f,*]

[a] Advanced Center for Chronic Diseases (ACCDiS), Facultad Ciencias Quimicas y Farmaceuticas & Facultad de Medicina, Universidad de Chile, Santiago 8380453, Chile
[b] Center for Studies of Exercise, Metabolism and Cancer (CEMC), Facultad de Medicina, Universidad de Chile, Santiago 8380453, Chile
[c] Programa de Fisiología y Biofísica, Instituto de Ciencias Biomédicas, Facultad de Medicina, Universidad de Chile, Chile
[d] Escuela de Kinesiologia, Facultad de Medicina, Universidad Finis Terrae, Santiago, Chile
[e] Department of Morphology, Surgery and Experimental Medicine, Section of Pathology, Oncology and Experimental Biology, Laboratory for Technologies of Advanced Therapies (LTTA), University of Ferrara, Ferrara, Italy
[f] Division of Cardiology, Department of Internal Medicine, University of Texas Southwestern Medical Center, Dallas, TX, USA

ARTICLE INFO

Keywords:
Inositol triphosphate receptor
Mitochondria
Autophagy
Mitophagy
Skeletal muscle
Muscle dystrophy

ABSTRACT

Duchenne muscular dystrophy (DMD) is characterized by a severe and progressive destruction of muscle fibers associated with altered Ca^{2+} homeostasis. We have previously shown that the IP_3 receptor (IP_3R) plays a role in elevating basal cytoplasmic Ca^{2+} and that pharmacological blockade of IP_3R restores muscle function. Moreover, we have shown that the IP_3R pathway negatively regulates autophagy by controlling mitochondrial Ca^{2+} levels. Nevertheless, it remains unclear whether IP_3R is involved in abnormal mitochondrial Ca^{2+} levels, mitochondrial dynamics, or autophagy and mitophagy observed in adult DMD skeletal muscle. Here, we show that the elevated basal autophagy and autophagic flux levels were normalized when IP_3R was downregulated in mdx fibers. Pharmacological blockade of IP_3R in mdx fibers restored both increased mitochondrial Ca^{2+} levels and mitochondrial membrane potential under resting conditions. Interestingly, mdx mitochondria changed from a fission to an elongated state after IP_3R knockdown, and the elevated mitophagy levels in mdx fibers were normalized. To our knowledge, this is the first study associating IP_3R1 activity with changes in autophagy, mitochondrial Ca^{2+} levels, mitochondrial membrane potential, mitochondrial dynamics, and mitophagy in adult mouse skeletal muscle. Moreover, these results suggest that increased IP_3R activity in mdx fibers plays an important role in the pathophysiology of DMD. Overall, these results lead us to propose the use of specific IP_3R blockers as a new pharmacological treatment for DMD, given their ability to restore both autophagy/mitophagy and mitochondrial function.

1. Introduction

The inositol 1,4,5-trisphosphate receptor (IP_3R) is an endoplasmic reticulum (ER) channel that regulates the release of Ca^{2+} from intracellular stores [1,2] upon binding of the second messenger IP_3, which is produced after activation of various cell plasma membrane receptors by extracellular signals [3,4]. Three isoforms of the receptor have been described (type 1, type 2, and type 3), all of which can modulate a large number of cellular processes, including cell death and survival [5]. Our previous work has shown that IP_3R is required for normal skeletal muscle activity, exerting its effects by regulating gene expression, energy metabolism, and mitochondrial activity [6–11]. Moreover, we described a novel mechanism for IP_3 generation in skeletal muscle through activation of P2Y metabotropic purinergic receptors by extracellular ATP, released through a pannexin 1/voltage sensor Cav1.1-dependent mechanism [6,12,13]. We also showed that this mechanism acts as an anti-apoptotic signal in normal skeletal muscle fibers after depolarization but fails to do so in dystrophic mouse fibers [8,14].

Duchenne muscular dystrophy (DMD) is caused by the absence of functional dystrophin [15,16]. In normal skeletal muscle, dystrophin is associated with a complex of glycoproteins known as dystrophin-

* Corresponding authors at: Advanced Center for Chronic Diseases (ACCDiS), Facultad Ciencias Quimicas y Farmaceuticas & Facultad de Medicina, Universidad de Chile, Santiago 8380453, Chile.
E-mail addresses: dvalladares@med.uchile.cl (D. Valladares), slavander@uchile.cl (S. Lavandero).

https://doi.org/10.1016/j.bbadis.2018.08.042
Received 5 May 2018; Received in revised form 6 August 2018; Accepted 30 August 2018
Available online 07 September 2018
0925-4439/

associated proteins, providing a link between the extracellular matrix and cytoskeleton [17]. The absence of dystrophin leads to progressive muscle weakening [18]. Ca^{2+} homeostasis is altered in DMD [19], and the disease is characterized by muscle fiber loss due to activation of Ca^{2+}-dependent proteases [20–22]. We and other groups have shown that IP_3R plays a role in the elevated basal levels of cytoplasmic Ca^{2+} characteristic of dystrophic muscle cells [23–28]. Furthermore, IP_3R expression is altered in both dystrophic human and dystrophic mouse muscle cells [25,29,30]. Pharmacological blockade of IP_3R decreases basal Ca^{2+} levels, corrects Ca^{2+} release upon stimulation, reduces mitochondrial Ca^{2+}, and restores muscle function [23,26,31]. Over the past years, a number of pharmacological treatments that target Ca^{2+} homeostasis have been proposed for DMD treatment [19]. More recently, some reports have suggested that regulation of another Ca^{2+}-dependent process, autophagy, could be a novel target for DMD treatment [32–37].

Autophagy is a conserved catabolic cellular process by which a cell degrades its own components, including long-lived proteins, protein aggregates, and dysfunctional organelles [38]. This process often occurs in response to nutrient deprivation but can also be triggered by other external stimuli [39]. Autophagy generally protects mammalian cells from death, and a defective autophagic response — whether deficient or elevated — is associated with various pathologies [39–41]. In skeletal muscle cells, autophagy is required for myoblast differentiation [42], muscle mass maintenance [43], muscle adaptation to exercise [44], and other processes. Impaired autophagy has been observed in muscle atrophy [45], aging [46], various myopathies [47], and in muscle samples of mdx mice and DMD patients [32–34,37].

In our previous work, we showed that the IP_3/IP_3R signaling pathway negatively regulates autophagy by interacting with the Beclin1/Bcl2 complex [48,49] and/or inducing changes in cytosolic and/or mitochondrial Ca^{2+} levels [50,51]. Nevertheless, to date there has been no detailed study on IP_3R-regulated autophagy, either in normal adult skeletal muscle fibers or DMD muscle fibers.

When autophagy selectively targets mitochondria for degradation, the process is termed mitophagy [52]. Defective mitochondria are delivered to the lysosome [53]. Interestingly, mitophagy also appears to be involved in pathological skeletal muscle conditions such as atrophy, aging, and some muscular dystrophies [54]. Mitochondrial dysfunction is a well-established finding in DMD [55–57]. IP_3R is found in the mitochondria-associated sarcoplasmic membranes (MAM), where it controls the Ca^{2+} exchange between the ER and mitochondria and regulates mitochondrial function and dynamics [58–60]. Nevertheless, it remains unclear whether the IP_3R is involved in the altered mitochondrial Ca^{2+} levels, mitochondrial dynamics, and mitophagy observed in adult DMD skeletal muscle.

Therefore, the present study was designed to investigate the role of the IP_3 receptor in the dysregulated mitochondrial function and altered autophagy/mitophagy levels observed in the skeletal muscle of mdx mice.

2. Materials and methods

2.1. Animals

All animal procedures were performed in accordance with the guidelines of the Bioethics Committee of the Facultad Medicina, Universidad de Chile (FONDECYT #3140491). All animals were obtained from the Animal Facility of the Facultad Medicina, Universidad de Chile, Santiago, Chile. The animals were euthanized by cervical dislocation. The *flexor digitorum brevis* (FDB) muscles were dissected from 5- to 8-week-old male *mdx* mice and wild-type C57Bl/6J mice and frozen in liquid nitrogen or stored at 80 °C until use.

2.2. Electroporation in vivo

Mice were anesthetized with 2% isoflurane and subjected to the protocol described by Di Franco et al. [61]. Briefly, animals were subcutaneously injected with 10 μL of hyaluronidase (2 mg/mL) in each footpad. One hour later, the animals were anesthetized a second time and injected with the plasmid sh-Scrambled in the left footpad and $shIP_3R1$ in the right footpad (5–10 μg/μL, OriGene, #TR517036). For some experiments 2mtGCaMP6m (Dr. Paolo Pinton, University of Ferrara) or MitoDsRed (Takara Bio Inc., #632421) were also injected in each footpad. Animals were allowed to recover for 15 min. Finally, the mice were anesthetized again and electroporated with one acupuncture needle under the skin at the heel and a second needle at the base of the toes, applying 20 pulses, 20 ms in duration each, at 1 Hz. After 2 weeks, the animals were euthanized. Successful transfection was confirmed using a microscope coupled to a fluorescence system (SMZ 1500, Nikon), and IP_3R1 downregulation was measured by real-time PCR (Suppl. Fig. 1). We have previously shown the successful transfection for 2mtGCaMP6m and MitoDsRed by fluorescence microscopy and IP_3R1 downregulation by Western blot [62].

2.3. Adult FDB fiber isolation

Isolated fibers from the *flexor digitorum brevis* (FDB) muscle were obtained by enzymatic digestion with collagenase type IV (2.7 mg/mL; Worthington Biochemicals Corp., Lakewood, NJ, USA) for 90 min at 37 °C followed by mechanical dissociation with fire-polished Pasteur pipettes. Isolated fibers were seeded in ECM gel dishes (Sigma #E1270) with DMEM (Gibco, Invitrogen, 12800-017), supplemented with 10% horse serum. Fibers were used for analysis 20 h after seeding.

2.4. Western blot

Total FDB muscle samples were lysed using an electric homogenizer (Fluko, Shanghai, China) in a lysis buffer as previously described [63]. The lysis buffer used to analyze IP_3R1 content contained: 20 mM Na3VO4, 1 mM PMSF, 1 mM BAPTA, 1 mM EDTA, 1 mM EGTA, T-PER, and protease inhibitors (Complete Mini, Roche Applied Science, #11836153001). Protein quantification was performed with a bicinchoninic acid protein assay (BCA) kit (Pierce, Rockford, IL, USA). Proteins were separated using SDS-PAGE and transferred to PVDF membranes. Primary antibodies were incubated overnight at 4 °C and secondary antibodies for 1 h at room temperature. Antibodies and dilutions were as follows: LC3-I/II (1:1000; Cell Signaling #2775S), p62 (1:5000; Abnova #H00008878-M01), Cox IV (1:1000; Cell Signaling #4850), p-DRP1 (Ser637) (1:1000; Cell Signaling #4867), DRP1 (1:1000; Thermo Scientific #PA1–16987), Fis1 (1:1000; Enzo Life Sciences #ALX-210-1037), Pink1 (1:1000; Abcam #ab23707), Parkin (1:1000; Millipore #MAB5512), α-tubulin (1:5000; Cell Signaling #2144), mouse IgG-HRP (1:20,000; Thermo Scientific, #31430), and anti-rabbit IgG-HRP (1:30,000; Thermo Scientific, #31460). The protein bands in the blots were visualized using a WESTAR Supernova detection kit (Cyanagen, Bologna, Italy), and the intensity of the bands was determined with ImageJ densitometry analysis.

2.5. mRNA isolation, cDNA, and real-time PCR

mRNA isolation, cDNA preparation, and real-time PCR were performed as previously described [63] using the primers listed in Suppl. Table 1.

2.6. Immunofluorescence studies

Isolated fibers were fixed with 4% paraformaldehyde (Electron Microscopy Science, Hatfield, PA, USA) in PBS for 15 min at 37 °C. Cells were rinsed with PBS and incubated with 100 mM glycine for 10 min.

Fibers were then permeabilized with 0.1% Triton X-100. Fibers were blocked with 0.1% saponin and 8% goat serum in PBS and incubated with primary antibody overnight at 4 °C (Parkin 1:250; Millipore #MAB5512). Finally, the cells were washed with PBS and incubated with Alexa Fluor 488 secondary antibody (Invitrogen, #A11001) for 2 h and washed again. The samples were mounted in Dako anti-fading reactive (Dako, Denmark) before microscopy.

2.7. Mitochondrial calcium measurement

Muscle fibers were isolated after 14 days of electroporation with mtGcamP6m and with or without shIP$_3$R1. The real-time imaging was evaluated using an inverted Olympus IX81 microscope with a 40×/N.A. 1.3 oil-immersion objective. The mtGcamP6m plasmid was stimulated at two excitation wavelengths λexc1/λexc2: 400/490 nm (80 ms of exposure each), and images were detected through a 460/15–525/25 nm. Ca^{2+} levels were expressed as a ratio of the emission to 490 and 400 nm (490/400 nm fluorescence ratio). The background was corrected using Image J filters (http://rsbweb.nih.gov/ij/).

2.8. Mitochondrial membrane potential measurement

Mitochondrial membrane potential was evaluated using tetramethylrhodamine ethyl ester ($TMRE^+$) in either non-quenching (20 nM) or quenching (400 nM) mode using a Carl Zeiss Pascal 5 LSM with a Plan Apo 60×/1.4 N.A. oil-immersion objective. In the non-quenching mode, 20 frames were collected for 1 s each, and the average fluorescence was quantified. In the quenching mode, the frames were collected each second and 50 frames were considered as a baseline. The cells were then stimulated with 1 μM FCCP (Sigma-Aldrich, #C2920) to induce mitochondrial membrane potential collapse, and the fluorescence of the cytoplasm was measured. The background was corrected frame-by-frame using an ImageJ filter (NIH), and the results were expressed as $\Delta F/F_0$.

2.9. Statistical analysis

Statistical results for n experiments are expressed as mean ± SEM. A two-way repeated measures ANOVA was used to compare changes in protein levels and gene expression for every condition analyzed. If a significant main effect was found, a Fisher's least significant difference (LSD) test was then applied. A p-value < 0.05 was considered statistically significant.

3. Results

3.1. IP$_3$R1 knockdown normalizes basal autophagy levels in mdx fibers

Changes in IP$_3$R activity could have either positive or negative effects on autophagy, depending on the cell type and context [64]. To date, there have been no studies on the effect of IP$_3$R on autophagy in normal adult skeletal muscle, much less in a pathological condition such as DMD. To this aim, expression of key autophagy level markers was measured in wild-type and mdx fibers electroporated with a short-hairpin RNA that decreases IP$_3$R1 expression (Suppl. Fig. 1). The level of the lipidated form of the microtubule-associated protein-1 light chain 3 (LC3-II), which is produced during autophagosome formation, was higher in mdx than wild-type fibers ($p = 0.015$; Fig. 1A,B). After IP$_3$R knockdown, LC3-II levels dropped back to nearly normal levels in mdx fibers ($p = 0.018$), and no significant differences were observed in wild-type fibers. Similar results were obtained when the LC3-II/I ratio was measured as an indicator of active autophagy (Suppl. Fig. 2B). Interestingly, no changes were observed for LC3-I levels in any condition (Suppl. Fig. 2C). Levels of p62, a protein necessary for autophagosome formation, were also measured. p62 was higher under basal conditions in mdx fibers as compared to the wild-type ($p = 0.001$, Fig. 1C). After IP$_3$R1 knockdown, p62 levels in mdx fibers decreased ($p = 0.05$), and no significant differences were observed in wild-type fibers. Finally, LC3 and p62 expression levels were evaluated after IP$_3$R1 knockdown, as we have previously reported that this receptor modulates gene expression in skeletal muscle [65,66]. LC3 mRNA levels were higher in mdx than wild-type fibers ($p = 0.001$) (Fig. 1D). IP$_3$R1 knockdown induced increased LC3 mRNA levels in wild-type fibers ($p = 0.017$) but decreased levels in mdx fibers ($p = 0.001$). LC3 mRNA levels also tended to be lower in mdx than in wild-type fibers ($p = 0.06$). No differences between wild-type and mdx fibers were detected for basal p62 mRNA levels (Fig. 1E). p62 levels increased after IP$_3$R1 knockdown in wild-type but not mdx fibers. These results suggest that IP$_3$R1 activity increases basal autophagy in mdx fibers and that IP$_3$R knockdown restores LC3 and p62 levels in these cells.

3.2. Basal autophagic flux is elevated in dystrophic fibers and normalized after IP$_3$R1 knockdown

To evaluate autophagic flux, fibers from wild-type and mdx mice were incubated for 3 h with 30 nM chloroquine, an autophagosome degradation blocker (Fig. 1). Under basal conditions, LC3-II levels were markedly increased in the mdx fibers after chloroquine incubation ($p = 0.007$) (Fig. 1A,B). When fibers were electroporated with shIP$_3$R1 and incubated with chloroquine, no changes in LC3-II levels were detected in wild-type fibers. Nevertheless, shScramble treated wild-type fibers showed higher LC3-II levels than shIP$_3$R1 treated wild-type fibers after incubation with chloroquine ($p = 0.015$, Fig. 1B). In mdx fibers, the effect of chloroquine was blocked when fibers were electroporated with shIP$_3$R1 ($p = 0.001$). Results for the LC3-II/I ratio were similar (Suppl. Fig. 2B); no significant changes in LC3-I levels were observed (Suppl. Fig. 2B), and incubation with chloroquine produced no significant changes in p62 levels in wild-type fibers under either plasmid condition (Fig. 1C). More interestingly, p62 levels decreased in both shScramble mdx ($p = 0.001$) and shIP$_3$R1 mdx fibers ($p = 0.003$) after chloroquine incubation, with no significant differences between the two groups. These results suggest that IP$_3$R1 modulates autophagic flux in both wild-type and mdx fibers. Moreover, IP$_3$R1 downregulation normalizes the elevated basal autophagic flux in mdx.

The accumulation of Ca^{2+} in the mitochondrial matrix has important implications for several processes, including autophagy [67]. Since we have previously shown that cytosolic Ca^{2+} was elevated in adult mdx fibers, we evaluated whether mitochondrial Ca^{2+} levels were also elevated in dystrophic fibers. As shown in Suppl. Fig. 3, basal Ca^{2+} fluorescence levels were about 1.5-fold higher in dystrophic than wild-type mitochondria ($p = 0.01$), measured using the mitochondrial ratiometric Ca^{2+} sensor 2mtGCaMP6m. Furthermore, when IP$_3$R1 activity was inhibited or its expression decreased, the basal Ca^{2+} fluorescence levels of the dystrophic mitochondria reached values similar to those of the wild-type mitochondria ($p = 0.02$ and $p = 0.01$, respectively). Finally, no changes were observed in basal Ca^{2+} levels in wild-type mitochondria when IP$_3$R1 activity was blocked (Suppl. Fig. 3A). Given that changes in mitochondrial Ca^{2+} could modulate the mitochondrial membrane potential (ΔΨm), which in turn modulates numerous critical mitochondrial functions [68], we assessed the effect of IP$_3$R inhibition on basal ΔΨm using the potentiometric dye TMRE in two modalities (see Materials and methods). Approximately two-fold increase in TMRE fluorescence was observed in the mdx mitochondria when this parameter was measured using TMRE in non-quenching mode ($p = 0.0005$, Suppl. Fig. 3B). Using two strategies for IP$_3$R inhibition, ΔΨm in the mdx fibers reached ΔΨm values in wild-type fibers (Xesto: $p = 0.043$; shIP$_3$R1: $p = 0.005$). In wild-type mitochondria, no significant differences in ΔΨm were found after IP$_3$R inhibition (Suppl. Fig. 3C). In agreement with these results, measurements with TMRE in quenching mode showed that ΔΨm depolarization of mdx cells with FCCP resulted in a larger transient increase in whole-cell fluorescence compared to the wild-type cells ($p = 0.001$, Suppl. Fig. 3D–E). Once

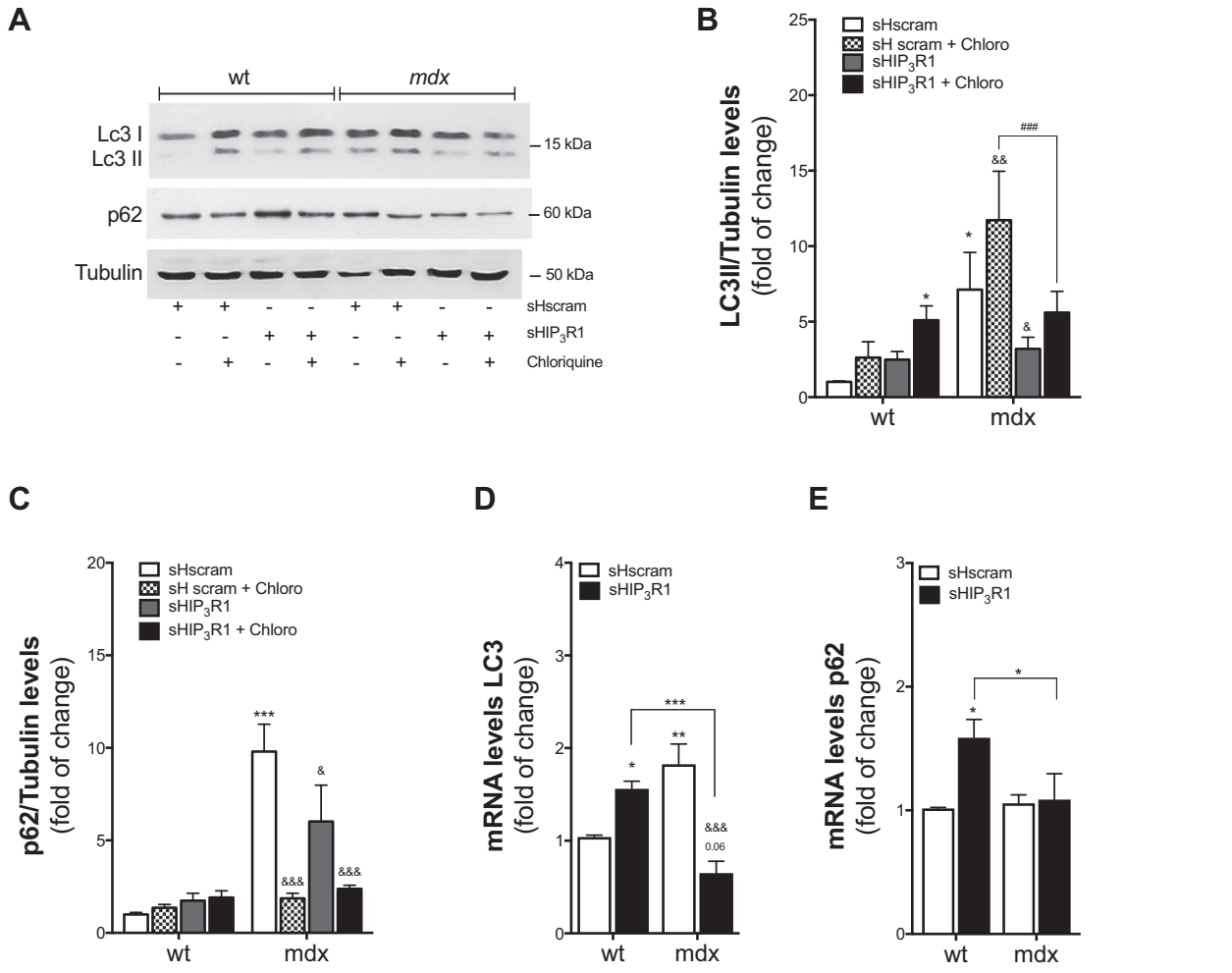

Fig. 1. IP_3R-dependent autophagic flux is increased in isolated muscle fibers from mdx mice.
(A–C) Representative immunoblot and quantification for LC3-II and p62 in isolated wild-type (wt) and mdx fibers electroporated with a scramble (shScram) or $shIP_3R1$ and treated with chloroquine (Chloro) for 3 h ($n = 4$). Tubulin was used as a loading control. (D, E) Relative amounts of the autophagy-related genes LC3 and p62 in isolated wild-type and mdx fibers electroporated with $shIP_3R1$ measured by real-time PCR ($n = 4$). Values are expressed as mean ± SEM. $^{*}p < 0.05$, $^{**}p < 0.01$, $^{***}p < 0.001$ versus wt shScram; $^{\&}p < 0.05$, $^{\&\&}p < 0.01$, $^{\&\&\&}p < 0.001$ versus mdx shScram.

again, IP_3R inhibition decreased the release of TMRE from mdx mitochondria, normalizing ΔΨm levels (Xesto: $p = 0.001$; $shIP_3R1$: $p = 0.001$). No effect of IP_3R inhibition on the ΔΨm of wild-type mitochondria was observed (Suppl. Fig. 3F).

3.3. IP_3R1 knockdown restores mitochondrial dynamics in mdx fibers

It is well established that mitochondria from mdx muscle fibers show altered functioning [57,69]. Nevertheless, few studies have addressed mitochondrial dynamics, and even fewer have investigated the role of IP_3R in these abnormalities. To evaluate mitochondrial network morphology, we used the mitochondrial marker MitoDsRed in wild-type and mdx fibers electroporated with $shIP_3R1$. The mitochondrial network morphology, visualized using confocal microscopy, revealed dramatic mitochondrial fragmentation in the mdx as compared to the wild-type fibers (Fig. 2A). Moreover, mdx fibers had three-fold the number of mitochondria as wild-type fibers ($p = 0.004$) and 10 times greater mitochondrial volume ($p = 0.004$, Fig. 2B), consistent with a more fragmented state. When IP_3R1 expression was decreased, the mitochondrial morphology of the mdx fibers shifted to a more fused state, and the number of mdx mitochondria were normalized to values near those of the wild-type cells ($p = 0.016$) (Fig. 2A, B). Nevertheless, no changes in mean mitochondrial volume were detected in mdx fibers after IP_3R downregulation. Interestingly, mitochondria from wild-type fibers did not show altered morphology after IP_3R downregulation (Fig. 2A, B).

To study which components of the mitochondrial fusion (Mtf2, Opa1) and fission (DRP1, Fis1) machinery mediate mitochondrial fragmentation in mdx fibers, real-time PCR analysis was performed. mRNA levels of the fusion mitochondria-associated proteins Mfn2 and Opa1 were similar in mdx and wild-type fibers, as were mRNA levels of the fission mitochondria-associated proteins DRP1 and Fis1 (Fig. 3A–D). We further tested the effects of IP_3R1 knockdown on the expression of mitochondrial dynamics proteins. After IP_3R1 knockdown, mRNA levels of Mfm2, DRP1, and Fis1 were decreased in mdx fibers, while Opa1 mRNA levels remained relatively unchanged (Fig. 3A–D). In wild-type fibers, Opa1 and Fis1 mRNA levels were significantly decreased; DRP1 mRNA was increased; and no changes were detected for Mfm2 mRNA after IP_3R1 knockdown. Second, when the levels of fission proteins DRP1 and Fis1 were measured, only phospho-DRP1 was found to be significantly higher in mdx than wild-type fibers (Fig. 3E–F). More interestingly, after IP_3R1 knockdown, phospho-DRP1 levels were significantly decreased in mdx fibers but elevated in wild-type fibers (Fig. 3F). Fis1 protein mRNA levels were decreased after IP_3R1 knockdown in both wild-type and mdx fibers (Fig. 3E, G). Finally, we evaluated expression of Cox IV as an indicator of mitochondrial biogenesis (Fig. 3E, H). No difference in Cox IV expression was found between wild-type and mdx fibers, suggesting that

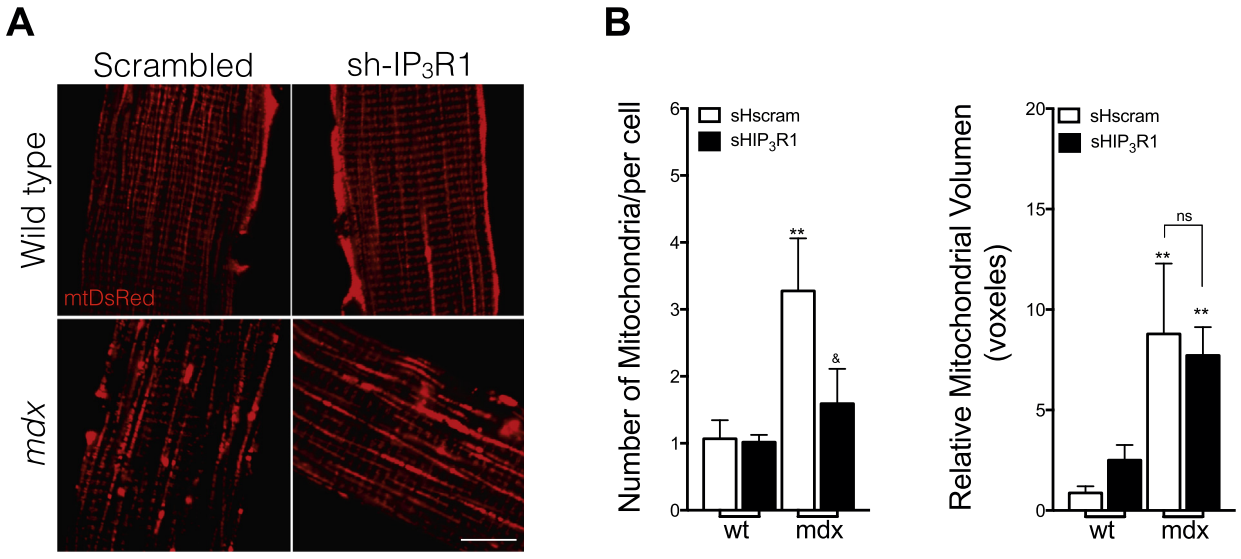

Fig. 2. IP_3R1 knockdown reestablishes mitochondrial network morphology and dynamics in isolated muscle fibers from mdx mice.
(A) Representative images of 1 μm confocal slices of mitochondrial network organization visualized with mitoDsRed in isolated wild-type and mdx fibers electroporated with shScram or $shIP_3R1$. Scale bar is 10 μm (B) Mitochondrial number and volume of the fibers as described in A ($n = 4$). Values are mean ± SEM. $^{**}p < 0.01$ versus wt shScram; $^{\&}p < 0.05$ versus mdx shScram.

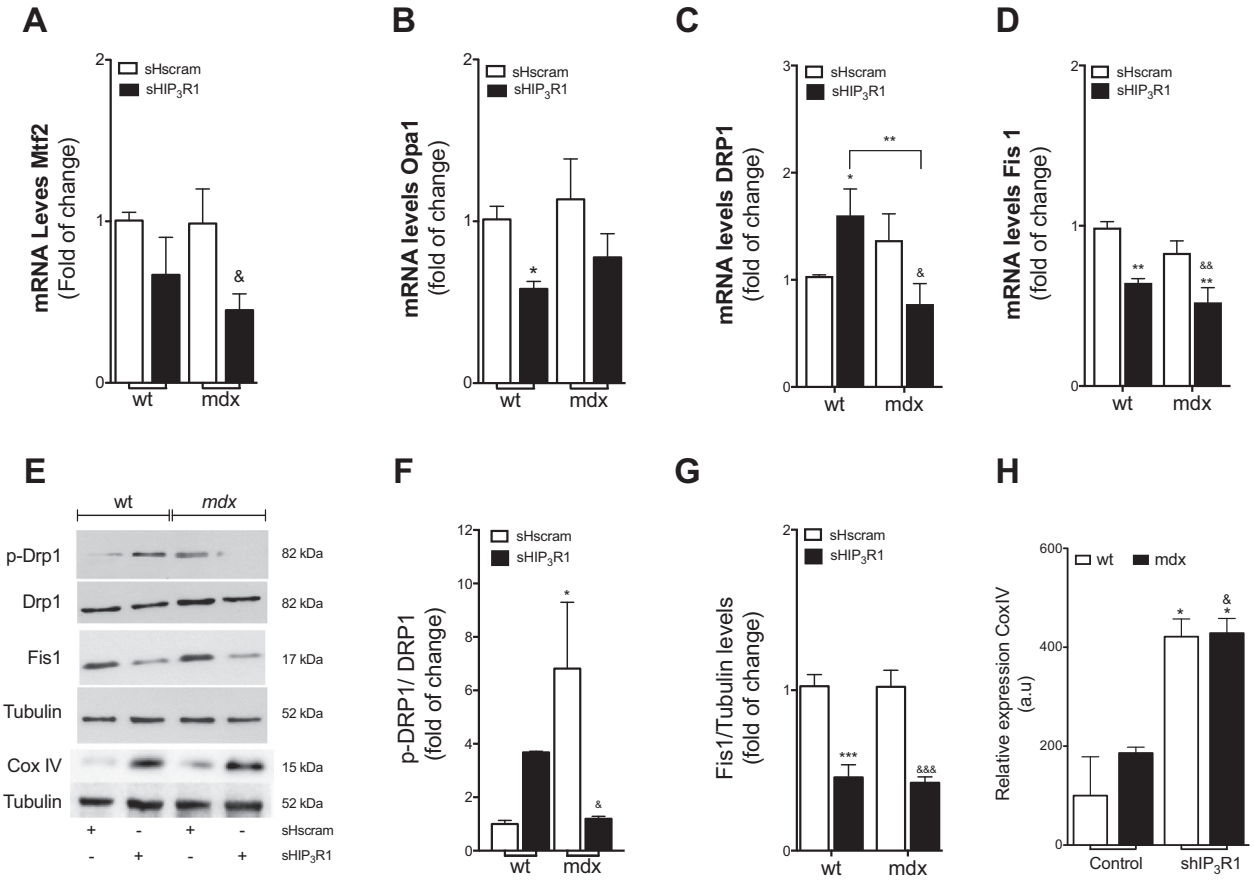

Fig. 3. IP_3R1 differentially regulates the expression pattern of proteins related to mitochondrial dynamics in isolated muscle fibers from wild-type and mdx mice. (A–D) Gene expression of mitochondrial dynamics proteins measured by real-time PCR ($n = 4$). (E–H) Representative Western blot and measurements of the fission proteins and Cox IV in isolated wild-type and mdx fibers electroporated with $shIP_3R1$ ($n = 4$). Values are mean ± SEM. $^{*}p < 0.05$, $^{**}p < 0.01$, $^{***}p < 0.001$ versus wt shScram; $^{\&}p < 0.05$, $^{\&\&}p < 0.01$, $^{\&\&\&}p < 0.001$ versus mdx shScram.

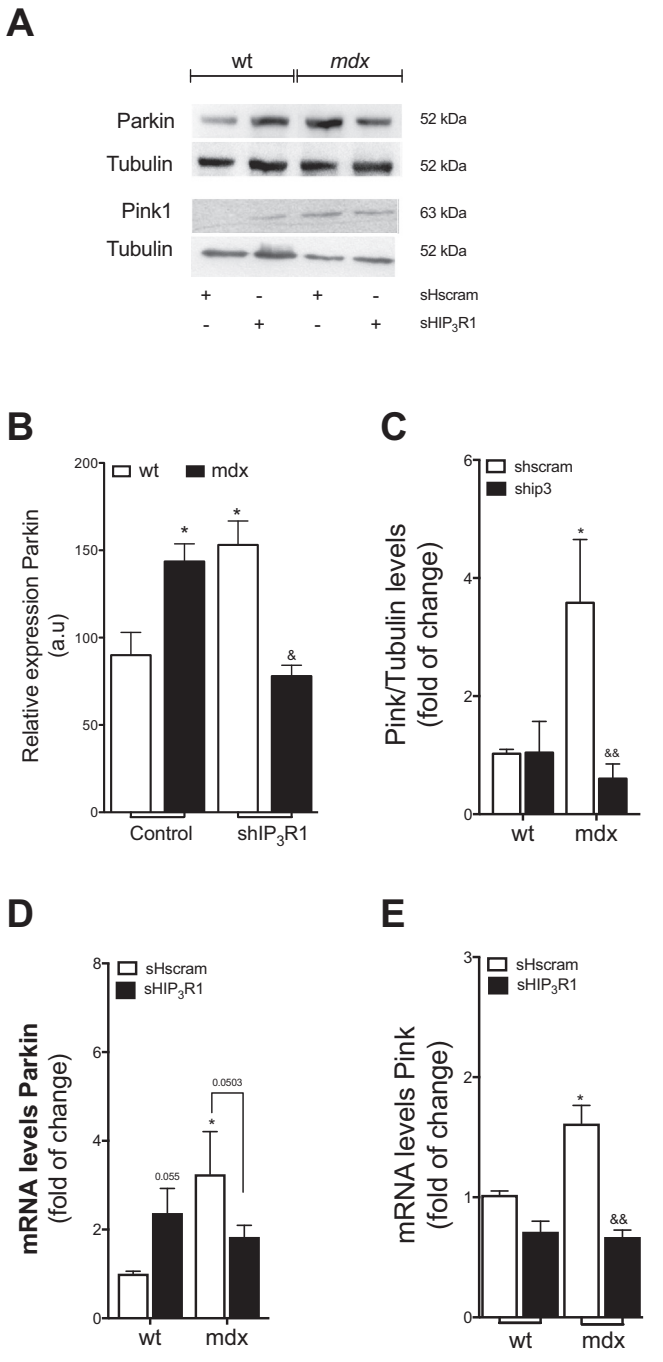

Fig. 4. IP_3R1 regulates the expression of proteins related to mitophagy in isolated muscle fibers from wild-type and mdx mice.
(A–C) Representative Western blot and Parkin and Pink1 measurements in isolated wild-type and mdx fibers electroporated with $shIP_3R1$ ($n = 4$). (D–E) Parkin and Pink1 gene expression measured by real-time PCR ($n = 4$). Values are mean ± SEM. $^{*}p < 0.05$ versus wt shScram; $^{\&}p < 0.05$, $^{\&\&}p < 0.01$ versus mdx shScram.

changes in mitochondrial dynamics but not mitochondrial biogenesis occur in mdx fibers. Additionally, Cox IV protein levels increased greatly after IP_3R1 knockdown in both fiber types (Fig. 3H), implying that IP_3R1 can somehow regulate mitochondrial biogenesis in both wild-type and mdx fibers.

3.4. Mitophagy is decreased after IP_3R1 knockdown in dystrophic fibers

Mitochondrial damage is mitigated through various defensive strategies, including activation of mitophagy, which acts as an important mechanism for controlling mitochondrial turnover [70]. Given that mdx mitochondria have a more fragmented morphology (Fig. 3) and higher intracellular Ca^{2+} levels (Supl. 3), it would be reasonable to hypothesize that mitophagy levels might be elevated in mdx fibers. Therefore, we evaluated the expression of two mitophagy-related proteins, Pink1 and Parkin, and assessed whether IP_3R1 knockdown could alter the expression of these proteins. Interestingly, Parkin protein expression was increased in mdx compared to wild-type fibers ($p = 0.003$), while IP_3R1 knockdown decreased Parkin expression ($p = 0.015$, Fig. 4A, B). In wild-type fibers, Parkin protein expression was increased after IP_3R1 knockdown ($p = 0.03$, Fig. 4B). Mdx fibers also showed increased levels of Pink1 expression as compared to wild-type fibers ($p = 0.02$), and IP_3R1 knockdown restored Pink1 normal levels ($p = 0.01$, Fig. 4A, C). mRNA levels for both Pink1 ($p = 0.006$) and Parkin ($p = 0.02$) were increased in mdx as compared to wild-type fibers (Fig. 4D, E). Moreover, IP_3R1 knockdown decreased the expression of both Pink1 ($p = 0.001$) and Parkin ($p = 0.05$) proteins in mdx fibers, while in wild-type fibers, only Parkin levels increased ($p = 0.055$, Fig. 4D, E).

When mitophagy is activated, Pink1 is stabilized in the mitochondrial membrane, triggering Parkin recruitment and activation [71]. Therefore, we evaluated Parkin localization by immunofluorescence before and after IP_3R1 knockdown in wild-type and mdx fibers (Fig. 5). In the wild-type fibers, Parkin was localized homogenously throughout the fiber (Fig. 5A, B). Remarkably, in the mdx fibers, Parkin was localized mainly in the sub-sarcolemmal area, while in knockdown fibers the distribution was fairly homogenous, similar to the wild-type fibers (Fig. 5A, B). Interestingly, IP_3R1 knockdown induces Parkin distribution in wild-type fibers that is similar to that observed in mdx fibers (Fig. 5A, B).

4. Discussion

DMD, the most common form of childhood muscular dystrophy, is characterized by rapidly progressive muscle weakness and wasting due to degeneration of skeletal muscle. Alteration in Ca^{2+} homeostasis has been proposed as a mechanism of DMD pathogenesis. In the present study, we evaluated the participation of IP_3R1 in basal autophagy, autophagic flux, mitochondrial Ca^{2+}, mitochondrial membrane potential, mitochondrial dynamics, and mitophagy in adult skeletal fibers. Moreover, we showed that IP_3R1 knockdown or a pharmacological antagonist restored nearly all of the parameters that are abnormal in adult mdx skeletal fibers. In addition, we also showed that in wild-type fibers, IP_3R1 knockdown induces changes in mitochondrial dynamics and mitophagy. To the best of our knowledge, this is the first study in adult mouse skeletal muscle associating IP_3R1 activity with changes in autophagy, mitochondrial dynamics, and mitophagy.

Several recent reports have proposed that modulation of autophagy is a promising novel therapy for DMD [33,34,37,72,73]. Nevertheless, some results have been controversial, and many questions remain to be addressed. Several groups have found depressed autophagy after measuring LC3 and p62 levels in mdx fibers [33–35,74]. On the contrary, our results showed increased LC3-II and p62 levels in mdx as compared to wild-type fibers. These results are consistent with those reported by two other groups [32,37]. The main difference between our study and the others was the age of the mdx mice used to assess autophagy levels. We used mdx mice between 5 and 8 weeks of age, whereas the other groups evaluated mice older than 16 weeks. In agreement with our findings, Fiacco et al. showed that LC3-II levels were higher in 6-week-old mdx mice than wild-type mice and that this increase gradually declines from 20 through 24–32 weeks in both the *tibialis anterior* and diaphragm muscles (Fig. 1) [37]. Moreover, this group also found

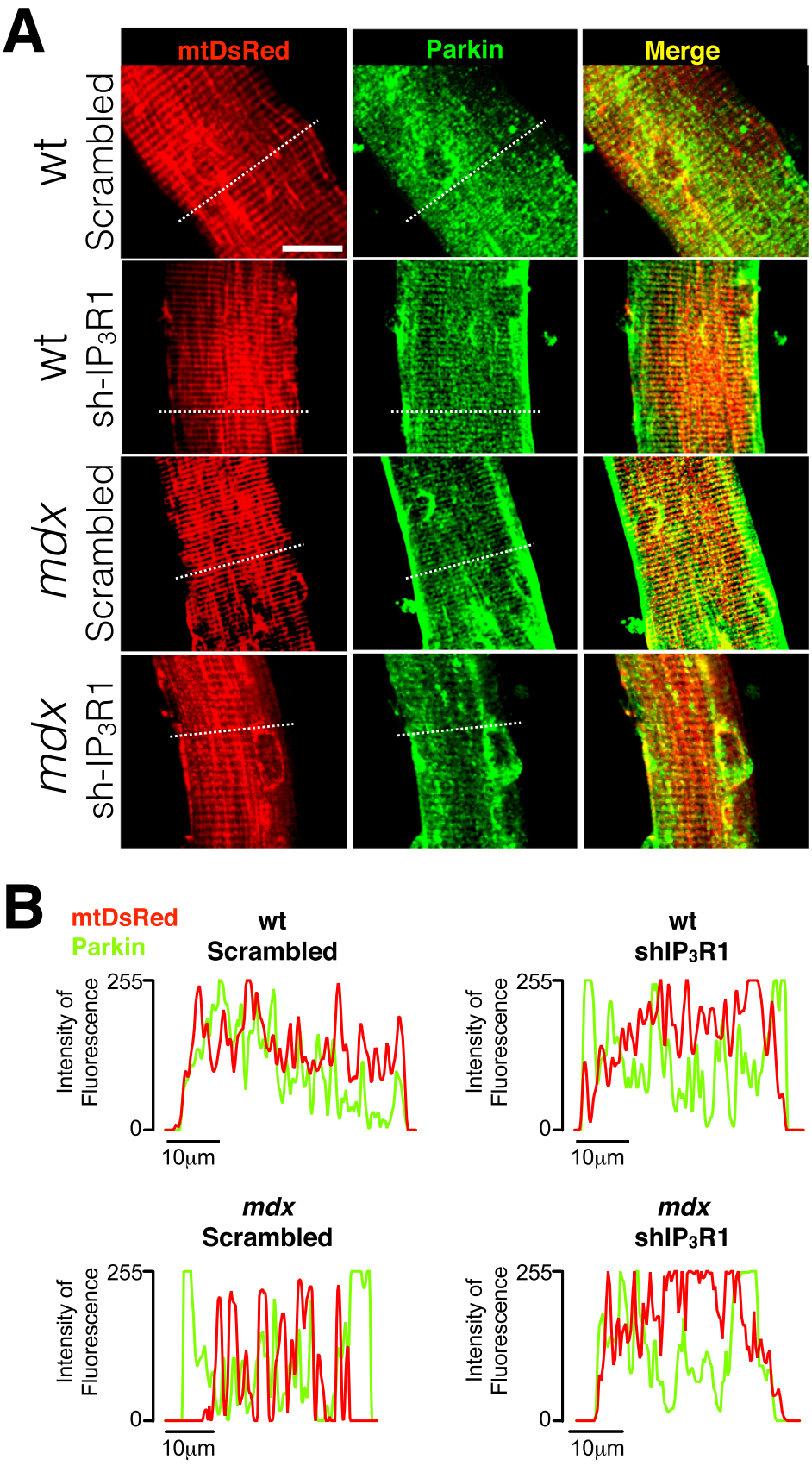

Fig. 5. Localization of the mitophagy proteins Parkin in isolated muscle fibers from mdx mice changes after IP_3R1 knockdown.
(A) Representative confocal immunofluorescence images for Parkin in wild-type and mdx *FDB*-isolated fibers electroporated with specific mitochondrial matrix MitoDsRed and with $shIP_3R1$ ($n = 3$). (B) Protein distribution at the fiber *z*-axis was performed by line scan and z-projection reconstruction. Quantitation of fluorescence intensity in the area marked with a *white square* is shown under each image. Scale bars = 10 μm.

elevated LC3 levels in muscle biopsies from DMD patients. Levels were highest during early stages (2 years), declining in later stages (8 years) [37]. Finally, Wattin et al. described elevated LC3 levels in myotubes from DMD patients [75]. We also found that autophagic flux is higher in mdx than wild-type fibers after incubation with the autophagosome degradation blocker chloroquine (Fig. 1). Similar results were obtained in young mdx mice were injected with chloroquine for 4 consecutive days; young mdx mice were injected with AICAR, an AMPK activator, for 4 weeks; and myotubes from DMD patients incubated with a cocktail of lysosomal protease inhibitors [37,75]. In older mdx mice, chloroquine treatment or starvation failed to induce changes in autophagic flux [33,37]. Only nanoparticles loaded with rapamycin, an autophagy inducer, has been found to increase autophagic flux in older mdx mice [74]. The differences in autophagy levels observed could be explained by the well-defined stages of mdx in mice. At 3 weeks of age, processes such as necrosis, apoptosis, and inflammation begin to emerge. Around 6 weeks, regeneration is initiated, continuing until 12 weeks of age and alternating with degeneration processes. The cycles of necrosis and regeneration are slower and milder after 12 weeks [76]. Finally, at 20 weeks, fibrosis begins, increasing at later stages [37]. The muscle pathology is mostly pronounced between 2 and 8 weeks of age. Therefore, we chose mice of this age to study autophagy [77]. Collectively, these results suggest that autophagy and flux levels depend on the progress of the disease and may be related to changes in regeneration and fibrosis [37].

Recently, IP_3R has emerged as a novel autophagy regulator that acts through several mechanisms, such as changes in cytosolic and/or mitochondrial Ca^{2+} levels [48]. Moreover, depending on the cell type, this receptor may either activate or inhibit autophagy [64]. Our results showed that IP_3R1 activity increased basal autophagy levels in mdx fibers, with autophagy restored to wild-type levels after IP_3R1 knockdown (Fig. 1). In addition, mdx fibers showed elevated levels of autophagic flux, which was also reduced after IP_3R1 knockdown (Fig. 1). Moreover, we found that changes in IP_3R1 activity induced changes in the mRNA levels of LC3 and p62. Surprisingly, some of these changes were not reflected in the protein levels in both wild-type and mdx fibers. Stoughton et al. showed a decrease in the mRNA levels of LC3 in golden retriever muscular dystrophy model (GRMD) in both *cranial sartorius* (CS) and *vastus lateralis* (VL) muscle. Nevertheless, the protein level of LC3 was increased in CS with no changes in VL muscle in GRMD [78]. Similar results were also observed for autophagy induction by starvation in myotonic dystrophy type I [79] and for the effect of aerobic exercise training in spontaneously hypertensive rats [80]. Further research is required to elucidate these contrasting patterns of autophagy protein expression induced by IP_3R1 knockdown in skeletal muscle.

The localization of IP_3R on the MAM allows it to modulate autophagy through the Ca^{2+} exchange between the ER and mitochondria and to influence mitochondrial function and dynamics. Our results suggest that IP_3R1 is involved in mitochondrial network morphology and dynamics characteristic of adult mdx skeletal fibers (Figs. 2, 3). It is well known that mitochondrial function is altered in dystrophic fibers [57,69]. Nevertheless, little is known about the participation of IP_3R in these mitochondrial alterations. Some studies have shown abnormal mitochondrial fragmentation in the *Caenorhabditis elegans* and zebrafish models of DMD, similar to our results in adult mdx skeletal fibers (Fig. 2) [81,82]. Moreover, Giacomotto et al. demonstrated the involvement of cytochrome *c* in muscle fiber death in *C. elegans* DMD models, in part through an interaction with IP_3R [81]. Additionally, this group also showed that knockdown of both DRP1 and IP_3R resulted in fewer muscle cells with fragmented mitochondria in the dystrophic *C. elegans* cells as compared to controls. Our results support these findings. We propose that IP_3R1 knockdown modulates mitochondrial dynamics by decreasing expression of both DRP1 and Fis1 in adult mdx fibers (Fig. 3). More interestingly, we found changes in the expression of fission proteins in wild-type fibers after IP_3R1 knockdown that were independent of changes in mitochondrial dynamics.

Mitophagy has emerged as a key mechanism in cell quality control, responsible for the elimination of damaged mitochondria [83]. Accumulating evidence has emphasized that mitochondrial fragmentation is a requirement for mitophagy [84]. Our results showed that mdx fibers show increased levels of mitophagy, reflected in the elevated expression of the two key mitophagy proteins, Pink and Parkin (Fig. 4). Additionally, Parkin was mainly localized in the sub-sarcolemmal area in mdx fibers, whereas Parkin distribution is fairly homogenous throughout the cell in wild-type fibers (Fig. 5). These results suggest that mitochondria that localized in the sub-sarcolemmal area could be more susceptible to mitophagy. This proposal is consistent with ultrastructural analyses that revealed a 39% decrease in sub-sarcolemmal mitochondrial density in mdx skeletal muscle fibers, with no significant changes in total mitochondria content [82]. Sub-sarcolemmal mitochondria not only regulate ATP production and Ca^{2+} handling but also contribute to glucose homeostasis, fat metabolism, and muscle adaptation to exercise [5,44,45]. Recent results from our group showed that depolarization-induced mitochondrial Ca^{2+} signals begin in the sub-sarcolemmal mitochondria then propagate towards the intermyofibrillar mitochondria [62]. Due to the importance of sub-sarcolemmal mitochondrial activity, we propose that the reduced numbers of these mitochondria, attributable to mitophagy, could play a role in several characteristic features of mdx fibers, including Ca^{2+} mishandling and decreased ATP energy supply. In accordance with our latest results, the decrease in sub-sarcolemmal mitochondria may also affect intermyofibrillar mitochondria function in mdx fibers [62]. IP_3R1 knockdown in mdx fibers decreased Parkin expression and restored Parkin localization to a distribution similar to that found in wild-type fibers (Fig. 5). Conversely, decreased IP_3R1 expression in wild-type fibers increased Parkin levels and increased Parkin localization to the sub-sarcolemmal area, similar to the distribution found in mdx fibers. These results show that IP_3R1 is necessary for normal mitochondrial function in skeletal muscle.

As mentioned previously, IP_3R may either activate or inhibit autophagy depending on the cell type through changes in cytosolic and/or mitochondrial Ca^{2+} levels [48]. In agreement with our results, Basset et al. showed that carbachol-induced mitochondrial Ca^{2+} responses are higher in the dystrophic myotubes of young mdx mice than those obtained from wild-type mice [85]. Moreover, these authors proposed that Bcl2 overexpression may prevent mitochondrial Ca^{2+} overload and Ca^{2+}-dependent apoptosis by inhibiting IP_3R in dystrophic myotubes [85]. These results together suggest that the flux of Ca^{2+} from IP_3Rs to the mitochondrial matrix could be a plausible mechanism for autophagy regulation in skeletal muscle. Moreover, this mechanism could also be important for mitophagy response. MacVicar et al. identified IP3Rs as mediators of Parkin-induced mitophagy in human RPE1 cells [86]. They showed an impaired mitophagy phenotype in cells suppressed for all three IP3R isoforms and for the mitochondrial Ca^{2+} uniporter (MCU) [86]. Although there is no direct evidence, these results suggest that mitophagy could be regulated by modulators of mitochondrial Ca^{2+}. Nevertheless, further research is needed to establish a direct relation between IP_3R1 activity and modulation of autophagy/mitophagy, through regulation of mitochondrial Ca^{2+} content in normal and mdx skeletal muscle fibers.

5. Conclusion

The results of this study emphasize the role of IP_3R in skeletal muscle function, especially in DMD. To our knowledge, this is the first evidence showing the involvement of IP_3R in autophagy, mitophagy, and mitochondrial function in adult mdx skeletal fibers. Nevertheless, several questions remain to be addressed, such as how IP_3R regulates these processes in both wild-type and adult mdx skeletal fibers. Several mechanisms have been proposed for the regulation of IP_3R activity, including changes in Bcl2 and Beclin1 levels [48,49]; constitutive IP_3R

activation by cleavage, triggered by caspases or calpains [87,88]; and disruption of ER/mitochondria communication, mediated by the interaction of IP_3R and Grp75/VDAC [89]. More research is needed to elucidate the exact mechanism by which IP_3R activity deregulates such processes in adult mdx skeletal fibers.

Finally, we previously showed that treating mdx mice with nifedipine, a DHPR blocker that indirectly decreases IP_3 levels, improved several features of mdx pathophysiology such as CK levels, cytoplasmic calcium levels, and expression of genes with apoptosis [31]. These results, along with those obtained here, lead us to propose the use of specific IP_3R blockers as a new pharmacological treatment for DMD, given their ability to simultaneously restore autophagy, mitophagy, and mitochondrial function in dystrophic skeletal muscle tissue.

Transparency document

The transparency document associated with this article can be found in the online version.

Acknowledgements

This work was supported by grants from the Fondo Nacional de Desarrollo Científico y Tecnologico (FONDECYT) grants 1161156 to S.L., 3140491 to D.V., 1151293 to E.J., 11130267 to A.C-F, CONICYT AT-21150604 to AD-V, and FONDAP 15130011 to S.L. P.P. is supported by the Italian Ministry of Education, University and Research; the Italian Ministry of Health; Telethon (GGP15219/B); the Italian Association for Cancer Research (AIRC: IG-18624); and by local funds from the University of Ferrara. S.M. is supported by “Fondazione Umberto Veronesi” and the Italian Ministry of Health.

Appendix A. Supplementary data

Supplementary data associated with this article can be found in the online version, at doi: https://doi.org/10.1016/j.bbadis.2018.08.042.

References

[1] J.K. Foskett, C. White, K.-H. Cheung, D.-O.D. Mak, Inositol trisphosphate receptor Ca^{2+} release channels, Physiol. Rev. 87 (2007) 593–658, https://doi.org/10.1152/physrev.00035.2006.

[2] K. Mikoshiba, IP 3 receptor/Ca^{2+} channel: from discovery to new signaling concepts, J. Neurochem. 102 (2007) 1426–1446, https://doi.org/10.1111/j.1471-4159.2007.04825.x.

[3] M.J. Berridge, The inositol trisphosphate/calcium signaling pathway in health and disease, Physiol. Rev. 96 (2016) 1261–1296, https://doi.org/10.1152/physrev.00006.2016.

[4] O.A. Fedorenko, E. Popugaeva, M. Enomoto, P.B. Stathopulos, M. Ikura, I. Bezprozvanny, Intracellular calcium channels: inositol-1,4,5-trisphosphate receptors, Eur. J. Pharmacol. 739 (2014) 39–48, https://doi.org/10.1016/j.ejphar.2013.10.074.

[5] H. Ivanova, T. Vervliet, L. Missiaen, J.B. Parys, H. De Smedt, G. Bultynck, Inositol 1,4,5-trisphosphate receptor-isoform diversity in cell death and survival, BBA-Mol. Cell. Res. 1843 (2014) 2164–2183, https://doi.org/10.1016/j.bbamcr.2014.03.007.

[6] G. Jorquera, F. Altamirano, A. Contreras-Ferrat, G. Almarza, S. Buvinic, V. Jacquemond, E. Jaimovich, M. Casas, Cav1.1 controls frequency-dependent events regulating adult skeletal muscle plasticity, J. Cell Sci. 126 (2013) 1189–1198, https://doi.org/10.1242/jcs.116855.

[7] A. Díaz-Vegas, C.A. Campos, A. Contreras-Ferrat, M. Casas, S. Buvinic, E. Jaimovich, A. Espinosa, ROS production via P2Y1-PKC-NOX2 is triggered by extracellular ATP after electrical stimulation of skeletal muscle cells, PLoS One 10 (2015) e0129882, , https://doi.org/10.1371/journal.pone.0129882.

[8] D. Valladares, G. Almarza, A. Contreras, M. Pavez, S. Buvinic, E. Jaimovich, M. Casas, Electrical stimuli are anti-apoptotic in skeletal muscle via extracellular ATP. Alteration of this signal in Mdx mice is a likely cause of dystrophy, PLoS One 8 (2013) e75340, , https://doi.org/10.1371/journal.pone.0075340.

[9] A. Contreras-Ferrat, P. Llanos, C. Vásquez, A. Espinosa, C. Osorio-Fuentealba, M. Arias-Calderon, S. Lavandero, A. Klip, C. Hidalgo, E. Jaimovich, Insulin elicits a ROS-activated and an IP_3-dependent Ca^{2+} release, which both impinge on GLUT4 translocation, J. Cell Sci. 127 (2014) 1911–1923, https://doi.org/10.1242/jcs.138982.

[10] A.E. Contreras-Ferrat, B. Toro, R. Bravo, V. Parra, C. Vásquez, C. Ibarra, D. Mears, M. Chiong, E. Jaimovich, A. Klip, S. Lavandero, An inositol 1,4,5-triphosphate (IP3)-IP3 receptor pathway is required for insulin-stimulated glucose transporter 4 translocation and glucose uptake in cardiomyocytes, Endocrinology 151 (2010) 4665–4677, https://doi.org/10.1210/en.2010-0116.

[11] C. Osorio-Fuentealba, A.E. Contreras-Ferrat, F. Altamirano, A. Espinosa, Q. Li, W. Niu, S. Lavandero, A. Klip, E. Jaimovich, Electrical stimuli release ATP to increase GLUT4 translocation and glucose uptake via PI3Kγ-Akt-AS160 in skeletal muscle cells, Diabetes 62 (2013) 1519–1526, https://doi.org/10.2337/db12-1066.

[12] S. Buvinic, G. Almarza, M. Bustamante, M. Casas, J. López, M. Riquelme, J.C. Sáez, J.P. Huidobro-Toro, E. Jaimovich, ATP released by electrical stimuli elicits calcium transients and gene expression in skeletal muscle, J. Biol. Chem. 284 (2009) 34490–34505, https://doi.org/10.1074/jbc.M109.057315.

[13] M. Arias-Calderón, G. Almarza, A. Díaz-Vegas, A. Contreras-Ferrat, D. Valladares, M. Casas, H. Toledo, E. Jaimovich, S. Buvinic, Characterization of a multiprotein complex involved in excitation-transcription coupling of skeletal muscle, Skelet. Muscle 6 (2016) 15, , https://doi.org/10.1186/s13395-016-0087-5.

[14] D. Valladares, F. Altamirano, C. Henríquez-Olguín, M. Casas, J.R. López, P.D. Allen, E. Jaimovich, Nifedipine treatment reduces resting calcium concentration, oxidative and apoptotic gene expression, and improves muscle function in dystrophic mdx mice, PLoS One 8 (2013) e81222, , https://doi.org/10.1371/journal.pone.0081222.

[15] D.J. Blake, A. Weir, S.E. Newey, K.E. Davies, Function and genetics of dystrophin and dystrophin-related proteins in muscle, Physiol. Rev. 82 (2002) 291–329, https://doi.org/10.1152/physrev.00028.2001.

[16] A.H. Ahn, L.M. Kunkel, The structural and functional diversity of dystrophin, Nat. Genet. 3 (1993) 283–291, https://doi.org/10.1038/ng0493-283.

[17] C.L. Batchelor, S.J. Winder, Sparks, signals and shock absorbers: how dystrophin loss causes muscular dystrophy, Trends Cell Biol. 16 (2006) 198–205, https://doi.org/10.1016/j.tcb.2006.02.001.

[18] A.E.H. Emery, The muscular dystrophies, Lancet 359 (2002) 687–695, https://doi.org/10.1016/S0140-6736(02)07815-7.

[19] A. Vallejo-Illarramendi, I. Toral-Ojeda, G. Aldanondo, A. López de Munain, Dysregulation of calcium homeostasis in muscular dystrophies, Expert Rev. Mol. Med. 16 (2014) e16, , https://doi.org/10.1017/erm.2014.17.

[20] P.R. Turner, T. Westwood, C.M. Regen, R.A. Steinhardt, Increased protein degradation results from elevated free calcium levels found in muscle from mdx mice, Nature 335 (1988) 735–738, https://doi.org/10.1038/335735a0.

[21] M.A. Badalamente, A. Stracher, Delay of muscle degeneration and necrosis in mdx mice by calpain inhibition, Muscle Nerve 23 (2000) 106–111 http://www.ncbi.nlm.nih.gov/pubmed/10590413.

[22] M.J. Spencer, Overexpression of a calpastatin transgene in mdx muscle reduces dystrophic pathology, Hum. Mol. Genet. 11 (2002) 2645–2655, https://doi.org/10.1093/hmg/11.21.2645.

[23] H. Balghi, S. Sebille, L. Mondin, A. Cantereau, B. Constantin, G. Raymond, C. Cognard, Mini-dystrophin expression down-regulates IP3-mediated calcium release events in resting dystrophin-deficient muscle cells, J. Gen. Physiol. 128 (2006) 219–230, https://doi.org/10.1085/jgp.200609559.

[24] F. Altamirano, J.R. López, C. Henríquez, T. Molinski, P.D. Allen, E. Jaimovich, Increased resting intracellular calcium modulates NF-κB-dependent inducible nitric-oxide synthase gene expression in dystrophic mdx skeletal myotubes, J. Biol. Chem. 287 (2012) 20876–20887, https://doi.org/10.1074/jbc.M112.344929.

[25] C. Cárdenas, N. Juretić, J. a Bevilacqua, I.E. García, R. Figueroa, R. Hartley, A.L. Taratuto, R. Gejman, N. Riveros, J. Molgó, E. Jaimovich, Abnormal distribution of inositol 1,4,5-trisphosphate receptors in human muscle can be related to altered calcium signals and gene expression in Duchenne dystrophy-derived cells, FASEB J. 24 (2010) 3210–3221, https://doi.org/10.1096/fj.09-152017.

[26] L. Mondin, H. Balghi, B. Constantin, C. Cognard, S. Sebille, Negative modulation of inositol 1,4,5-trisphosphate type 1 receptor expression prevents dystrophin-deficient muscle cells death, Am. J. Phys. Cell Physiol. 297 (2009) C1133–C1145, https://doi.org/10.1152/ajpcell.00048.2009.

[27] N. Juretic, G. Jorquera, P. Caviedes, E. Jaimovich, N. Riveros, Electrical stimulation induces calcium-dependent up-regulation of Neuregulin-1β in dystrophic skeletal muscle cell lines, Cell. Physiol. Biochem. 29 (2012) 919–930, https://doi.org/10.1159/000188068.

[28] C. Henríquez-Olguín, F. Altamirano, D. Valladares, J.R. López, P.D. Allen, E. Jaimovich, Altered ROS production, NF-κB activation and interleukin-6 gene expression induced by electrical stimulation in dystrophic mdx skeletal muscle cells, Biochim. Biophys. Acta 1852 (2015) 1410–1419, https://doi.org/10.1016/j.bbadis.2015.03.012.

[29] A. Farini, C. Sitzia, L. Cassinelli, F. Colleoni, D. Parolini, U. Giovanella, S. Maciotta, A. Colombo, M. Meregalli, Y. Torrente, Inositol 1,4,5-trisphosphate (IP3)-dependent Ca2+ signaling mediates delayed myogenesis in Duchenne muscular dystrophy fetal muscle, Development 143 (2016) 658–669, https://doi.org/10.1242/dev.126193.

[30] J.L. Liberona, J.A. Powell, S. Shenoi, L. Petherbridge, R. Caviedes, E. Jaimovich, Differences in both inositol 1,4,5-trisphosphate mass and inositol 1,4,5-trisphosphate receptors between normal and dystrophic skeletal muscle cell lines, Muscle Nerve 21 (1998) 902–909 http://www.ncbi.nlm.nih.gov/pubmed/9626250.

[31] F. Altamirano, D. Valladares, C. Henriquez-Olguin, M. Casas, J.R. Lopez, P.D. Allen, E. Jaimovich, Nifedipine treatment reduces resting calcium concentration, oxidative and apoptotic gene expression, and improves muscle function in dystrophic mdx mice, PLoS One 8 (2013) e81222, , https://doi.org/10.1371/journal.pone.0081222.

[32] M. Pauly, F. Daussin, Y. Burelle, T. Li, R. Godin, J. Fauconnier, C. Koechlin-Ramonatxo, G. Hugon, A. Lacampagne, M. Coisy-Quivy, F. Liang, S. Hussain, S. Matecki, B.J. Petrof, AMPK activation stimulates autophagy and ameliorates muscular dystrophy in the mdx mouse diaphragm, Am. J. Pathol. 181 (2012)

583–592, https://doi.org/10.1016/j.ajpath.2012.04.004.
[33] C. De Palma, F. Morisi, S. Cheli, S. Pambianco, V. Cappello, M. Vezzoli, P. Rovere-Querini, M. Moggio, M. Ripolone, M. Francolini, M. Sandri, E. Clementi, Autophagy as a new therapeutic target in Duchenne muscular dystrophy, Cell Death Dis. 3 (2012) e418, https://doi.org/10.1038/cddis.2012.159.
[34] R. Pal, M. Palmieri, J.A. Loehr, S. Li, R. Abo-Zahrah, T.O. Monroe, P.B. Thakur, M. Sardiello, G.G. Rodney, Src-dependent impairment of autophagy by oxidative stress in a mouse model of Duchenne muscular dystrophy, Nat. Commun. 5 (2014) 4425, , https://doi.org/10.1038/ncomms5425.
[35] P. Spitali, P. Grumati, M. Hiller, M. Chrisam, A. Aartsma-Rus, P. Bonaldo, Autophagy is impaired in the tibialis anterior of dystrophin null mice, PLOS Curr. (2013), https://doi.org/10.1371/currents.md.e1226cefa851a2f079bbc406c0a21e80.
[36] M. Sandri, L. Coletto, P. Grumati, P. Bonaldo, Misregulation of autophagy and protein degradation systems in myopathies and muscular dystrophies, J. Cell Sci. 126 (2013) 5325–5333, https://doi.org/10.1242/jcs.114041.
[37] E. Fiacco, F. Castagnetti, V. Bianconi, L. Madaro, M. De Bardi, F. Nazio, A. D'Amico, E. Bertini, F. Cecconi, P.L. Puri, L. Latella, Autophagy regulates satellite cell ability to regenerate normal and dystrophic muscles, Cell Death Differ. 23 (2016), https://doi.org/10.1038/cdd.2016.70.
[38] N. Mizushima, B. Levine, A.M. Cuervo, D.J. Klionsky, Autophagy fights disease through cellular self-digestion, Nature 451 (2008) 1069–1075, https://doi.org/10.1038/nature06639.
[39] P. Jiang, N. Mizushima, Autophagy and human diseases, Cell Res. 24 (2014) 69–79, https://doi.org/10.1038/cr.2013.161.
[40] D. Cervia, C. Perrotta, C. Moscheni, C. De Palma, E. Clementi, Nitric oxide and sphingolipids control apoptosis and autophagy with a significant impact on Alzheimer's disease, J. Biol. Regul. Homeost. Agents 27 (n.d.) 11–22. http://www.ncbi.nlm.nih.gov/pubmed/24813312.
[41] J.L. Schneider, A.M. Cuervo, Autophagy and human disease: emerging themes, Curr. Opin. Genet. Dev. 26 (2014) 16–23, https://doi.org/10.1016/j.gde.2014.04.003.
[42] F. Antigny, S. Konig, L. Bernheim, M. Frieden, Inositol 1,4,5 trisphosphate receptor 1 is a key player of human myoblast differentiation, Cell Calcium 56 (2014) 513–521, https://doi.org/10.1016/j.ceca.2014.10.014.
[43] E. Masiero, L. Agatea, C. Mammucari, B. Blaauw, E. Loro, M. Komatsu, D. Metzger, C. Reggiani, S. Schiaffino, M. Sandri, Autophagy is required to maintain muscle mass, Cell Metab. 10 (2009) 507–515, https://doi.org/10.1016/j.cmet.2009.10.008.
[44] V.A. Lira, M. Okutsu, M. Zhang, N.P. Greene, R.C. Laker, D.S. Breen, K.L. Hoehn, Z. Yan, Autophagy is required for exercise training-induced skeletal muscle adaptation and improvement of physical performance, FASEB J. 27 (2013) 4184–4193, https://doi.org/10.1096/fj.13-228486.
[45] E. Masiero, M. Sandri, Autophagy inhibition induces atrophy and myopathy in adult skeletal muscles, Autophagy 6 (2010) 307–309, https://doi.org/10.4161/auto.6.2.11137.
[46] D.C. Rubinsztein, G. Mariño, G. Kroemer, Autophagy and aging, Cell 146 (2011) 682–695, https://doi.org/10.1016/j.cell.2011.07.030.
[47] B.A. Neel, Y. Lin, J.E. Pessin, Skeletal muscle autophagy: a new metabolic regulator, Trends Endocrinol. Metab. 24 (2013) 635–643, https://doi.org/10.1016/j.tem.2013.09.004.
[48] A. Criollo, J.M. Vicencio, E. Tasdemir, M.C. Maiuri, S. Lavandero, G. Kroemer, The inositol trisphosphate receptor in the control of autophagy, Autophagy 3 (2007) 350–353 http://www.ncbi.nlm.nih.gov/pubmed/17404493.
[49] J.M. Vicencio, C. Ortiz, A. Criollo, A.W.E. Jones, O. Kepp, L. Galluzzi, N. Joza, I. Vitale, E. Morselli, M. Tailler, M. Castedo, M.C. Maiuri, J. Molgó, G. Szabadkai, S. Lavandero, G. Kroemer, The inositol 1,4,5-trisphosphate receptor regulates autophagy through its interaction with Beclin 1, Cell Death Differ. 16 (2009) 1006–1017, https://doi.org/10.1038/cdd.2009.34.
[50] C. Cárdenas, R.A. Miller, I. Smith, T. Bui, J. Molgó, M. Müller, H. Vais, K.-H. Cheung, J. Yang, I. Parker, C.B. Thompson, M.J. Birnbaum, K.R. Hallows, J.K. Foskett, Essential regulation of cell bioenergetics by constitutive InsP3 receptor Ca^{2+} transfer to mitochondria, Cell 142 (2010) 270–283, https://doi.org/10.1016/j.cell.2010.06.007.
[51] J.-P. Decuypere, K. Welkenhuyzen, T. Luyten, R. Ponsaerts, M. Dewaele, J. Molgó, P. Agostinis, L. Missiaen, H. De Smedt, J.B. Parys, G. Bultynck, Ins(1,4,5)P3 receptor-mediated Ca^{2+} signaling and autophagy induction are interrelated, Autophagy 7 (2011) 1472–1489 http://www.ncbi.nlm.nih.gov/pubmed/22082873.
[52] S.R. Yoshii, N. Mizushima, Autophagy machinery in the context of mammalian mitophagy, BBA-Mol. Cell. Res. 1853 ((2015) 2797–2801, https://doi.org/10.1016/j.bbamcr.2015.01.013.
[53] L.C. Gomes, L. Scorrano, Mitochondrial morphology in mitophagy and macroautophagy, BBA-Mol. Cell. Res. 1833 (2013) 205–212, https://doi.org/10.1016/j.bbamcr.2012.02.012.
[54] C.D. Katsetos, S. Koutzaki, J.J. Melvin, Mitochondrial dysfunction in neuromuscular disorders, Semin. Pediatr. Neurol. 20 (2013) 202–215, https://doi.org/10.1016/j.spen.2013.10.010.
[55] M. Onopiuk, W. Brutkowski, K. Wierzbicka, S. Wojciechowska, J. Szczepanowska, J. Fronk, H. Lochmüller, D.C. Górecki, K. Zabłocki, Mutation in dystrophin-encoding gene affects energy metabolism in mouse myoblasts, Biochem. Biophys. Res. Commun. 386 (2009) 463–466, https://doi.org/10.1016/j.bbrc.2009.06.053.
[56] M. Kelly-Worden, E. Thomas, Mitochondrial dysfunction in Duchenne muscular dystrophy, Open J. Endocr. Metab. Dis. 4 (2014) 211–218, https://doi.org/10.4236/ojemd.2014.48020.
[57] C.A. Timpani, A. Hayes, E. Rybalka, Revisiting the dystrophin-ATP connection: how half a century of research still implicates mitochondrial dysfunction in Duchenne muscular dystrophy aetiology, Med. Hypotheses 85 (2015) 1021–1033, https://doi.org/10.1016/j.mehy.2015.08.015.
[58] C. López-Crisosto, R. Bravo-Sagua, M. Rodriguez-Peña, C. Mera, P.F. Castro, A.F.G. Quest, B.A. Rothermel, M. Cifuentes, S. Lavandero, ER-to-mitochondria miscommunication and metabolic diseases, Biochim. Biophys. Acta Mol. basis Dis. 1852 ((2015) 2096–2105, https://doi.org/10.1016/j.bbadis.2015.07.011.
[59] C. Vásquez-Trincado, I. García-Carvajal, C. Pennanen, V. Parra, J.A. Hill, B.A. Rothermel, S. Lavandero, Mitochondrial dynamics, mitophagy and cardiovascular disease, J. Physiol. 594 (2016) 509–525, https://doi.org/10.1113/JP271301.
[60] S. Marchi, S. Patergnani, P. Pinton, The endoplasmic reticulum-mitochondria connection: one touch, multiple functions, Biochim. Biophys. Acta 1837 (2014) 461–469, https://doi.org/10.1016/j.bbabio.2013.10.015.
[61] M. Difranco, M. Quinonez, J. Capote, J. Vergara, DNA transfection of mammalian skeletal muscles using in vivo electroporation, J. Vis. Exp. (2009), https://doi.org/10.3791/1520.
[62] A.R. Díaz-Vegas, A. Cordova, D. Valladares, P. Llanos, C. Hidalgo, G. Gherardi, D. De Stefani, C. Mammucari, R. Rizzuto, A. Contreras-Ferrat, E. Jaimovich, Mitochondrial calcium increase induced by RyR1 and IP3R channel activation after membrane depolarization regulates skeletal muscle metabolism, Front. Physiol. 9 (2018) 791, , https://doi.org/10.3389/fphys.2018.00791.
[63] C. Henríquez-Olguín, A. Díaz-Vegas, Y. Utreras-Mendoza, C. Campos, M. Arias-Calderón, P. Llanos, A. Contreras-Ferrat, A. Espinosa, F. Altamirano, E. Jaimovich, D.M. Valladares, NOX2 inhibition impairs early muscle gene expression induced by a single exercise bout, Front. Physiol. 7 (2016) 282, , https://doi.org/10.3389/fphys.2016.00282.
[64] J.B. Parys, J.-P. Decuypere, G. Bultynck, Role of the inositol 1,4,5-trisphosphate receptor/Ca^{2+}-release channel in autophagy, Cell Commun. Signal 10 (2012) 17, https://doi.org/10.1186/1478-811X-10-17.
[65] J.A. Valdés, J. Hidalgo, J.L. Galaz, N. Puentes, M. Silva, E. Jaimovich, M.A. Carrasco, NF-kappaB activation by depolarization of skeletal muscle cells depends on ryanodine and IP3 receptor-mediated calcium signals, Am. J. Phys. Cell Physiol. 292 (2007) C1960–C1970, https://doi.org/10.1152/ajpcell.00320.2006.
[66] M. Casas, R. Figueroa, G. Jorquera, M. Escobar, J. Molgó, E. Jaimovich, IP(3)-dependent, post-tetanic calcium transients induced by electrostimulation of adult skeletal muscle fibers, J. Gen. Physiol. 136 (2010) 455–467, https://doi.org/10.1085/jgp.200910397.
[67] D.A. East, M. Campanella, Ca^{2+} in quality control: an unresolved riddle critical to autophagy and mitophagy, Autophagy 9 (2013) 1710–1719, https://doi.org/10.4161/auto.25367.
[68] M.R. Duchen, Mitochondria in health and disease: perspectives on a new mitochondrial biology, Mol. Asp. Med. 25 (2004) 365–451, https://doi.org/10.1016/j.mam.2004.03.001.
[69] E. Rybalka, C.T. Hons, Summary Report Duchenne Muscular Dystrophy as a Mitochondrial Myopathy: Why Therapeutically Targeting the Mitochondria Is a Plausible Treatment Avenue, (2015).
[70] V. Romanello, M. Sandri, Mitochondria quality control and muscle mass maintenace, Front. Physiol. 6 (2016) 422, , https://doi.org/10.3389/fphys.2015.00422.
[71] D.P. Narendra, S.M. Jin, A. Tanaka, D.-F. Suen, C.A. Gautier, J. Shen, M.R. Cookson, R.J. Youle, PINK1 is selectively stabilized on impaired mitochondria to activate Parkin, PLoS Biol. 8 (2010) e1000298, , https://doi.org/10.1371/journal.pbio.1000298.
[72] C. De Palma, C. Perrotta, P. Pellegrino, E. Clementi, D. Cervia, Skeletal muscle homeostasis in Duchenne muscular dystrophy: modulating autophagy as a promising therapeutic strategy, Front. Aging Neurosci. 6 (2014), https://doi.org/10.3389/fnagi.2014.00188.
[73] N.P. Whitehead, Enhanced autophagy as a potential mechanism for the improved physiological function by simvastatin in muscular dystrophy, Autophagy 12 (2016) 705–706, https://doi.org/10.1080/15548627.2016.1144005.
[74] K.P. Bibee, Y.-J. Cheng, J.K. Ching, J.N. Marsh, A.J. Li, R.M. Keeling, A.M. Connolly, P.T. Golumbek, J.W. Myerson, G. Hu, J. Chen, W.D. Shannon, G.M. Lanza, C.C. Weihl, S.A. Wickline, Rapamycin nanoparticles target defective autophagy in muscular dystrophy to enhance both strength and cardiac function, FASEB J. 28 (2014) 2047–2061, https://doi.org/10.1096/fj.13-237388.
[75] M. Wattin, L. Gaweda, P. Muller, M. Baritaud, C. Scholtes, C. Lozano, K. Gieseler, C. Kretz-Remy, Modulation of protein quality control and proteasome to autophagy switch in immortalized myoblasts from Duchenne muscular dystrophy patients, Int. J. Mol. Sci. 19 (2018) 178, https://doi.org/10.3390/ijms19010178.
[76] A. Nakamura, S. Takeda, Mammalian models of Duchenne muscular dystrophy: pathological characteristics and therapeutic applications, J Biomed Biotechnol 2011 (2011) 184393, https://doi.org/10.1155/2011/184393.
[77] R. Willmann, S. Possekel, J. Dubach-Powell, T. Meier, M. a Ruegg, Mammalian animal models for Duchenne muscular dystrophy, Neuromuscul. Disord. 19 (2009) 241–249, https://doi.org/10.1016/j.nmd.2008.11.015.
[78] W.B. Stoughton, J. Li, C. Balog-Alvarez, J.N. Kornegay, Impaired autophagy correlates with golden retriever muscular dystrophy phenotype, Muscle Nerve 10 (2018) e0119382, , https://doi.org/10.1002/mus.26121.
[79] M. Brockhoff, N. Rion, K. Chojnowska, T. Wiktorowicz, C. Eickhorst, B. Erne, S. Frank, C. Angelini, D. Furling, M.A. Rüegg, M. Sinnreich, P. Castets, Targeting deregulated AMPK/mTORC1 pathways improves muscle function in myotonic dystrophy type I, J. Clin. Invest. 127 (2017) 549–563, https://doi.org/10.1172/JCI89616.
[80] E.M. McMillan, M.-F. Paré, B.L. Baechler, D.A. Graham, J.W.E. Rush, J. Quadrilatero, Autophagic signaling and proteolytic enzyme activity in cardiac and skeletal muscle of spontaneously hypertensive rats following chronic aerobic exercise, PLoS One 10 (2015) e0119382, , https://doi.org/10.1371/journal.pone.

0119382.
[81] J. Giacomotto, N. Brouilly, L. Walter, M.-C. Mariol, J. Berger, L. Ségalat, T.S. Becker, P.D. Currie, K. Gieseler, Chemical genetics unveils a key role of mitochondrial dynamics, cytochrome c release and IP3R activity in muscular dystrophy, Hum. Mol. Genet. 22 (2013) 4562–4578, https://doi.org/10.1093/hmg/ddt302.
[82] J.M. Percival, M.P. Siegel, G. Knowels, D.J. Marcinek, Defects in mitochondrial localization and ATP synthesis in the mdx mouse model of Duchenne muscular dystrophy are not alleviated by PDE5 inhibition, Hum. Mol. Genet. 22 (2013) 153–167, https://doi.org/10.1093/hmg/dds415.
[83] D. Sebastián, A. Zorzano, Mitochondrial dynamics and metabolic homeostasis, Curr. Opin. Physiol. 3 (2018) 34–40, https://doi.org/10.1016/j.cophys.2018.02.006.
[84] G. Twig, A. Elorza, A.J.A. Molina, H. Mohamed, J.D. Wikstrom, G. Walzer, L. Stiles, S.E. Haigh, S. Katz, G. Las, J. Alroy, M. Wu, B.F. Py, J. Yuan, J.T. Deeney, B.E. Corkey, O.S. Shirihai, Fission and selective fusion govern mitochondrial segregation and elimination by autophagy, EMBO J. 27 (2008) 433 LP–446 http://emboj.embopress.org/content/27/2/433.abstract.
[85] O. Basset, F.-X. Boittin, C. Cognard, B. Constantin, U.T. Ruegg, Bcl-2 overexpression prevents calcium overload and subsequent apoptosis in dystrophic myotubes, Biochem. J. 395 (2006) 267–276, https://doi.org/10.1042/BJ20051265.
[86] T. MacVicar, L. Mannack, R. Lees, J. Lane, Targeted siRNA screens identify ER-to-mitochondrial calcium exchange in autophagy and mitophagy responses in RPE1 cells, Int. J. Mol. Sci. 16 (2015) 13356–13380, https://doi.org/10.3390/ijms160613356.
[87] R.J. Wojcikiewicz, J.A. Oberdorf, Degradation of inositol 1,4,5-trisphosphate receptors during cell stimulation is a specific process mediated by cysteine protease activity, J. Biol. Chem. 271 (1996) 16652–16655 http://www.ncbi.nlm.nih.gov/pubmed/8663308.
[88] R.L. Patterson, D. Boehning, S.H. Snyder, Inositol 1,4,5-trisphosphate receptors as signal integrators, Annu. Rev. Biochem. 73 (2004) 437–465, https://doi.org/10.1146/annurev.biochem.73.071403.161303.
[89] M. Pauly, C. Angebault-Prouteau, H. Dridi, C. Notarnicola, V. Scheuermann, A. Lacampagne, S. Matecki, J. Fauconnier, ER stress disturbs SR/ER-mitochondria Ca^{2+} transfer: implications in Duchenne muscular dystrophy, BBA-Mol. Basis Dis. 1863 (2017) 2229–2239, https://doi.org/10.1016/j.bbadis.2017.06.009.